Breast Cancer: Targets and Therapy

Dovepress
Taylor & Francis Group

Open Access Full Text Article

ORIGINAL RESEARCH

Exploratory Research of Intraductal Chemotherapy to Control the Focal Breast Lesion of Breast Cancer

Xin Lin[1], Xinzhuo Li[2], Qingping Wei[1], Hao Yuan[1], Ming Zhong[1], Jianlan Qiao[3], Jianzhong Gong[3], Yongping Li[4]

[1]Department of Breast Surgery, Shanghai Pudong Hospital, Fudan University Pudong Medical Center, Shanghai, 201399, People's Republic of China; [2]Fudan University, Shanghai, 200433, People's Republic of China; [3]Department of Radiology, Shanghai Pudong Hospital, Fudan University Pudong Medical Center, Shanghai, 201399, People's Republic of China; [4]Department of General Surgery of Shanghai Eighth People's Hospital, Shanghai, 200235, People's Republic of China

Correspondence: Yongping Li, Department of General surgery of Shanghai Eighth People's Hospital, Xuhui District, Shanghai, 200235, People's Republic of China, Tel +86 18930038167, Email liyongpingdt@sina.com; Jianzhong Gong, Department of Radiology, Shanghai Pudong Hospital, Fudan University Pudong Medical Center, 2800 Gongwei Road, Pudong New Area, Shanghai, 201399, People's Republic of China, Tel +8618918355119, Email 18918355119@163.com

Objective: The standard treatment for locally advanced breast cancer (LABC) is neoadjuvant therapy combined with surgery with chemotherapy as the main means. Elderly female patients often lose treatment opportunities due to the cardiotoxicity and other intolerable adverse reactions of chemotherapy drugs and their inoperability. Most breast cancers originate from the epithelial cells lining the ducts of the breast. We proposed that for the treatment of LABC, intraductal infusion of chemotherapeutic drugs could lead to high local exposure of the drug to the mammary ducts and avoid systemic toxicity. In order to verify its safety, we conducted a series of studies.

Methods: We perfused two different chemotherapeutic drugs into the mammary ducts of pigs or dogs, observed their skin toxicity and measured the drug distribution and concentration in tissues and blood. Strictly select clinical cases, perform intraductal chemotherapy, and observe their skin toxicity and systemic toxicity. In addition, drug transport pathways in the breast of Beagle dogs were clarified by combining contrast-enhanced magnetic resonance imaging (MRI) with gadolinium dimeglumine injection with advanced image processing techniques and computational fluid dynamics (CFD) simulations.

Results: In animal experiments, no grade II ~ IV skin toxicity related to perfusion drugs was observed. Strictly screened clinical cases significantly reduced tumor lesions by intraductal chemotherapy, and no significant cutaneous or systemic toxicity was observed. Validated models showed that the transport of contrast agent within the breast ducts mainly relies on convection and diffusion mechanisms, and convection shows a significantly higher transport efficiency than diffusion.

Conclusion: This study demonstrates the safety and feasibility of intraductal chemotherapy, provides preliminary data supporting the further investigation of intraductal chemotherapy as a potential local treatment strategy for LABC patients who cannot tolerate intravenous chemotherapy and cannot be operated on, and provides a valuable theoretical and computational basis for the selection of delivery routes and pharmacokinetic analysis of anticancer drugs.

Registration Details: This trial was approved by the Ethics Committee of Pudong Hospital Affiliated to Fudan University [Clinical Trial Number: (2021) Ethics Approval No. (QWJWZY-01)].

Keywords: intraductal administration, chemotherapy therapy, breast cancer, focal lesion

Introduction

Breast cancer over the age of 65 accounted for 34.3% in the world by 2022, and these elderly cases will increase by 56% between 2010 and 2030.[1–4] Locally advanced breast cancer (LABC) is present in approximately 8.5% of patients with breast cancer in the United States and 4% of patients with breast cancer in Europe.[5] LABC is usually treated with neoadjuvant therapy, which can downstage the primary breast tumor and metastatic lymph nodes to make them operable.[6] Neoadjuvant chemotherapy (NAC) is frequently used in neoadjuvant therapy, and others include endocrine therapy,

Received: 17 June 2025
Accepted: 18 November 2025
Published: 25 December 2025

targeted therapy and radiotherapy.[7–12] For older patients, chemotherapeutics or targeted drugs cannot be well tolerated, which caused cardiovascular toxicities and other adverse events.[13,14] Local treatment can improve these problems by reducing the systemic exposure of drugs.[15,16] Intramammary perfusion therapy has been used in breast diseases.

Most breast cancers originate from the epithelial cells lining the ducts of the breast.[17] The technique of ductal lavage was used to treat breast diseases by lavaging with drugs.[18–20] The medicine is delivered to the pathological tissue through the special sealed duct of the breast tissue, and directly acts on the lesion, avoids the medicine passing through the liver and intestine, reduces the side effects.[20] The Institute of Cancer Research, London, conducted a study by infusing breast specimens with high elastomer polyurethane (PU4ii resin).[21] Preclinical data showed that intraductal therapy, in which chemotherapy or another anticancer agent was delivered directly into a duct through the nipple, reached the end of catheter and prevented the development of breast malignancy.[22]

In the realm of breast cancer treatment, the anatomical complexity of the ductal structures plays a pivotal role, particularly when considering the feasibility of innovative retrograde drug delivery methods. Comprehensive studies utilizing Computational Fluid Dynamics (CFD) provided a profound insight into the fluid dynamics that milk transfer and drug delivery mechanisms within the breast. Twelves et al investigated the anatomical structure of ducts in breast cancer to optimize intraductal approaches for cytology and biomarker assessments, which were crucial for detecting pre-malignant changes within the ducts.[21] Mortazavi et al applied CFD to model the transport processes in lactating human breasts, utilizing clinically measured suckling pressures to simulate milk flow and intake dynamics.[23] This provided a unique perspective on the fluid dynamics within breast tissues under physiological conditions. Shipley et al developed a multiscale model to explore the fluid and drug distribution in vascular tumors, focusing on how vascular architecture influenced therapeutic efficacy, which highlighted the potential of computational models in optimizing chemotherapy delivery.[24] Wu et al utilized ultrafast dynamic contrast enhancement magnetic resonance imaging (DCE-MRI) to quantitatively analyze vascular properties, distinguishing between malignant and benign breast tumors through detailed hemodynamic profiling.[25] Further expanding on this, Wu et al developed patient-specific CFD models based on image-guided simulations to characterize breast cancer hemodynamics, enhancing the accuracy of treatment outcomes.[26] Additionally, Wu et al explored the optimization of neoadjuvant treatment protocols, employing CFD to tailor therapy approaches according to individual hemodynamic responses.[27]

This study introduced a novel approach to breast cancer treatment by leveraging the unique architecture of mammary ducts for targeted drug delivery, diverging significantly from traditional methods that rely predominantly on systemic routes. Intraductal chemotherapy has not been currently recommended by guidelines.[28] The problem is that local strategies can lead to skin necrosis of the nipples and breasts. The safety of preoperative intraductal chemotherapy for breast cancer needs to be evaluated and the pharmacokinetics effects of this treatment need to be examined. The study aims to demonstrate the safety of intraductal chemotherapy, and to determine the safe concentrations of chemotherapeutic drugs that can effectively downstage the tumor and lymph nodes. Unlike previous studies that employed CFD to understand drug delivery dynamics in generic settings, this research innovatively applied CFD to simulate the retrograde infusion process specifically within the mammary ducts. By mapping the potential pathways of drug transport directly through the ductal system, we have created a model that not only predicts the pharmacokinetic behavior of therapeutic agents but also minimizes systemic exposure, thereby reducing the likelihood of adverse side effects commonly associated with traditional chemotherapy. This tailored approach ensures high local drug concentrations at the tumor site, enhancing efficacy while safeguarding patient well-being. Furthermore, the use of advanced imaging and simulation techniques marks a significant improvement over earlier methodologies by providing a more accurate and detailed analysis of drug distribution and effects within the breast tissue.

Materials and Methods

Drugs and Instruments

PLD and Paclitaxel for Injection (Albumin bound) were purchased from China Shijiazhuang Pharmaceutical Group Co., Ltd. Tiletamine Hydrochloride and Zolazepam Hydrochloride was purchased from Shanghai Vic Trading Co., Ltd. Trastuzumab was purchased from Shanghai Fuhong Hanlin Biomedicine Co., Ltd. Precision Balance (ME104E) was

purchased from Mettle Toledo, Switzerland. Organization Crusher was purchased from Shanghai Jingxin Industrial Development Co., Ltd. High performance liquid chromatography (HPLC-1260) was purchased from Agilent, Japan. Liquid chromatography-mass spectrometry (LC-MS/MS-8060) was purchased from Shimadzu Company, Japan.

Detection of Doxorubicin

The Distribution of Adriamycin in Tissues Was Determined

After rinsing the tissue with normal saline, dry it and weigh it. 5% TritonX-100 (1mL/100mg) was added according to the weight, 4–5 grinding beads were added to each sample, and the tissue was crushed and homogenized by tissue crusher to make homogenization. Take 100μL tissue homogenate, add 100μL methanol solution containing internal standard daunorubicin hydrochloride (10μg/mL) to precipitate protein, 400μL chloroform to extract Adriamycin from tissue homogenate, after vortex 2min, 12000rpm centrifuge 5min at 4°C, absorb 200μL of lower solution into EP tube, and evaporate overnight at room temperature. After adding 100μL of 30% acetonitrile, vortex 2min and ultrasonic 15min, the supernatant was centrifuged and 10min at 4°C the supernatant was analyzed by HPLC. The peak areas of doxorubicin and daunorubicin were detected at fluorescence excitation wavelength 480nm and emission wavelength 550nm. A 5μm C18 column was used with 40% B liquid elution (A water containing 0.1% Trifluoroacetic acid and B acetonitrile containing 0.1% Trifluoroacetic acid), flow rate 0.7mL/min and injection volume 30μL. In addition, the doxorubicin solution was diluted with the blank homogenate of each tissue, and 100μL was used for the same operation, and the standard curve samples of each tissue were made, and the peak areas of doxorubicin and daunorubicin were detected. The ratio of peak area of doxorubicin to daunorubicin was used as ordinate, and the concentration of doxorubicin as Abscissa. The peak area ratio of each sample was substituted into the standard curve, and the concentration of doxorubicin in each tissue was calculated by converting dilution multiple.

The Concentration of Adriamycin in Blood Samples of Human or Pig Was Determined

HPLC method: 100μL plasma was diluted with 20μL normal saline, 100μL protein was precipitated in methanol solution containing internal standard daunorubicin hydrochloride (10μg/mL), 400μL chloroform extracted Adriamycin from plasma, after vortex 2min, 12000rpm centrifugation 5min at 4°C, 200μL of lower solution was absorbed into EP tube, and the ventilator was dried overnight at room temperature. After adding 100μL of 30% acetonitrile, vortex 2min and ultrasonic 15min, the supernatant was centrifuged and 10min at 4°C the supernatant was analyzed by HPLC. The peak areas of doxorubicin and daunorubicin were detected at fluorescence excitation wavelength 480nm and emission wavelength 550nm. A 5μm C18 column was used with 40% B liquid elution (A water containing 0.1% Trifluoroacetic acid and B acetonitrile containing 0.1% Trifluoroacetic acid), flow rate 0.7mL/min and injection volume 30μL. In addition, the solution of doxorubicin was diluted with blank blood sample gradient, and 100μL of doxorubicin was used to make the standard curve sample. The peak area of doxorubicin and daunorubicin was determined. The ratio of peak area of doxorubicin to daunorubicin was used as ordinate. The concentration of doxorubicin was used as Abscissa to draw the standard curve. The peak area ratio of each sample was substituted into the standard curve, and the concentration of doxorubicin in the blood sample was calculated by converting the dilution multiple.

LC-MS/MS method: when the detection limit was lower than the detection range of liquid phase (< 1μg/mL), LC-MS/MS was used to detect the concentration of doxorubicin in blood samples. 100μL plasma was diluted with 20μL normal saline, 100μL methanol solution containing internal standard daunorubicin hydrochloride (100ng/mL) to precipitate protein, 400μL chloroform to extract doxorubicin from plasma, vortex 2min, 12000rpm centrifugation 5min at 4°C, 200μL lower solution was absorbed into the EP tube, and the ventilator dried overnight at room temperature. After adding 100μL methanol-aqueous solution (v/v=1:1), vortex 2min and ultrasonic 15min, the supernatant was centrifuged and 10min at 4°C. 10μL of the supernatant was analyzed by LC-MS/MS. The ion pairs of doxorubicin and daunorubicin were 544.30 > 397.25 and 528.30 > 321.10, respectively. Using 3μm C18 column, the liquid phase condition is 2–8min16-34% B liquid gradient elution (A solution is water containing 0.1% formic acid, B liquid is acetonitrile), flow rate 0.3mL/min, injection volume 1μL. In addition, the solution of doxorubicin was diluted with blank blood sample gradient, and 100μL of doxorubicin was used to make the standard curve sample. The peak area of doxorubicin and daunorubicin was determined. The ratio of peak area of doxorubicin to daunorubicin was used as ordinate. The concentration of doxorubicin was used as Abscissa to draw the

standard curve. The peak area ratio of each sample was substituted into the standard curve, and the concentration of doxorubicin in the blood sample was calculated by converting the dilution multiple.

Animal Studies

In this study, the animal experiment was approved by the Animal Ethics Committee of Pudong Hospital Affiliated to Fudan University [No. 20211125–001], according to the ethics recommended in the Guidelines for Ethical Review of Laboratory Animal Welfare (GB/T35892-2018).

Bama Pig

Bama pigs, which had suckled, were anesthetized with Zoletil50 injection. The skin surface of nipples and surrounding was cleaned with alcohol swabs and air-dried. Then used a ductal probe to enlarge the breast ducts. Mammary ducts were cannulated with a number of 0.45mm duct irrigators. Drugs (PLD 10 mg dissolved in 10 mL 5% glucose solution, Albumin combined with paclitaxel 100mg dissolved in 20mL 0.9% sodium chloride solution) and equivalent placebos (15mL per treat) were, respectively, infused slowly into the mammary glands. After 2 hours, peripheral blood was sampled to measure drug concentration. Periodically observed the nipple and skin for redness, swelling, rupture, necrosis and other changes. A week later, second infusion was performed. Blood samples and biopsies were taken 2 hours after perfusion for concentration of drug as well. Tissue samples from the breast were obtained from central/periareolar, four peripheral samples 2cm away, at 12, 3, 6, and 9 O'clock, included skin and corresponding glandular tissue. Each tissue sample was snap-frozen in liquid nitrogen and kept in −80°C until analysis. The distribution of doxorubicin in tissues and blood was determined by HPLC-1260 and LC-MS/MS-8060. Finally, the curve of drug concentration in the blood and tissue were drawn.

Beagle Dog

Suckling beagle dogs were conducted in the same way as above. Agents included PLD injection (20mg, 5% glucose 5mL dilution, d1, d10) and paclitaxel for injection (albumin-bound) (100mg, 0.9% sodium chloride solution 20mL dilution, d1, d10). After perfusion, the drug distribution was measured as above.

Patients and Treatment

This trial strictly screened patients with non-operable LABC who could not tolerate systemic treatment or patients with locally recurrent breast cancer after breast-conserving surgery who could not tolerate systemic drug treatment after multiple lines of treatment. In this study, patients were enrolled and diagnosed at Shanghai Pudong Hospital. The Shanghai Pudong Hospital Ethics Committee was approved this study (No. QWJWZY-01). We obtained written informed consent to allow the sample collection and data analysis for research purposes, and to publish case details/images in the article.

Inclusion criteria: 1. Invasive breast cancer patients diagnosed by histopathology. 2. Tumor diameter greater than or equal to 5.0cm, one of the following three conditions: any age, unable to tolerate systemic chemotherapy, direct surgery and breast conservation, but strong desire for breast conservation; age over 70 years old, unable to direct surgery; tumor shrinkage after neoadjuvant chemotherapy is not obvious or local progression, or unable to tolerate neoadjuvant chemotherapy. 3. The tumor diameter is less than 5cm, and chemotherapy and surgery cannot be tolerated. Solid tumor evaluation can be performed. 4. Local recurrence of breast-conserving patients, local unresectable, or tumor size reduction is not obvious or progressive after systemic drug treatment. 5. HER2 positive. (Immunohistochemical test 3+ or in situ hybridization test positive), cannot tolerate targeted (double target) therapy and systemic chemotherapy; can tolerate targeted (double target) therapy, in accordance with the above 2–4. 6. The patient does not receive systemic chemotherapy. 7. The patient is not allowed to receive systemic chemotherapy for any reason. 8. Sign the informed consent form.

Exclusion criteria: 1. Patients who are allergic to or intolerant to local chemotherapy drugs or their excipients. 2. Patients with patency of breast ducts, drugs cannot pass through breast ducts. 3. Patients with recurrence of chest wall after mastectomy, drugs cannot be administered through breast ducts. 4. Patients with serious and uncontrollable systemic diseases. 5. Patients who are pregnant or lactating, or pregnant and puerperal safety cannot be guaranteed during study

treatment. 6. Patients who participate in other clinical trials at the same time. 7. Patients who are judged by the investigator to be unsuitable for participation in this study.

After disinfection and local anesthesia, we used a ductal probe to enlarge the breast ducts gently. Mammary ducts close to the lesion site were cannulated with a number of 0.45mm duct irrigators. Drugs and equivalent placebos were, respectively, infused slowly into the mammary glands at the same pressure and speed. Finally, the injectors were removed, and the nipples were covered with sterile dressing. Peripheral blood samples were collected 30 minutes before and 2 hours after infusion to detect doxorubicin concentration in plasma by LC-MS/MS. Based on the experience of clinicians, evaluated the efficacy and determined the timing of surgery. During the surgery, different parts of the breast, nipple, areola, and axillary lymph nodes were sampled, and sections were stained with DAPI (blue). The biodistribution of doxorubicin (red) was visualized by confocal laser scanning microscopy.

Galactography and Pharmacokinetic Simulation in Beagle Dogs

DCE-MRI Acquisition

In this study, gadopentetate dimeglumine was injected into the breast tissue of beagle dogs through the openings of the mammary ducts. After administering 5 mL of the contrast agent, the experimental animals were allowed to rest for 10 minutes.

MRI was performed at Shanghai Pudong Hospital using a GE Discovery MR750w system (manufactured by GE Healthcare Systems). Imaging was conducted using a three-dimensional spoiled gradient-recalled echo (3D GRE) protocol, which enhanced T1-weighted image contrast by applying spoiling gradients to eliminate steady-state signals, as shown in Figure 1a and b. Specific imaging parameters were carefully selected to optimize image quality. A flip angle of 15° was employed to enhance T1-weighted contrast. The repetition time (TR) was set at 6,496 ms, and the echo time (TE) was 1,742 ms to improve signal acquisition. A slice thickness of 1.4 mm, combined with an inter-slice spacing of 1.4 mm, provided detailed anatomical resolution. The in-plane spatial resolution achieved was 0.7031 × 0.7031 mm per pixel, allowing for high-definition imaging of the breast tissue. A temporal resolution of 57,559 ms was maintained to ensure comprehensive data collection within an acceptable time frame.

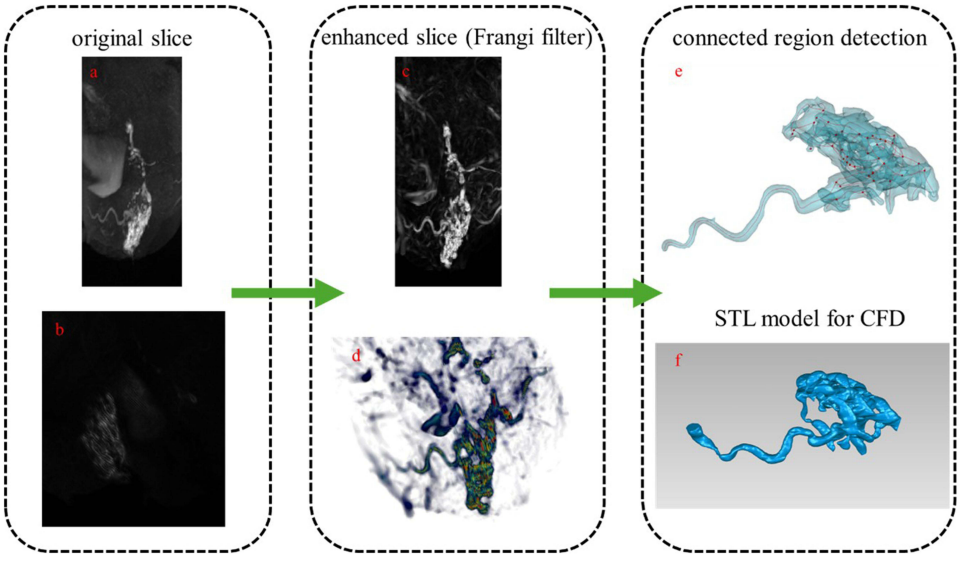

Figure 1 (**a**) depicts a slice of the original image, while (**b**) presents its three-dimensional reconstruction. (**c** and **d**) correspond to the enhanced slice and its respective three-dimensional reconstruction. (**e**) illustrates the schematic pathways obtained after connected component analysis; by retaining regions connected to the main duct, the computational domain (**f**) is obtained.

https://doi.org/10.2147/BCTT.S547684

Vessel Enhancement and Segmentation

Threshold segmentation and the Frangi filter were employed in this study to enhance the accuracy of imaging recognition of breast duct features.[25–27] Initially, MATLAB software was used to read and process the MRI image data. The image data were first normalized to reduce noise and artifacts introduced by imaging inconsistencies, specifically by adjusting the brightness and contrast of the images to achieve standardization. Here, I_{min} and I_{max} represent the manually calibrated minimum and maximum threshold values, respectively, and the grayscale values were normalized to the interval [0, 1]:

$$I = \begin{cases} 0, I_{min} \\ \frac{I-I_{min}}{I_{max}-I_{min}}, I_{min}<I<I_{max} \\ 1, I>I_{max} \end{cases}$$

By performing a Taylor expansion of the normalized image in its local neighborhood, the coefficient matrix of the second-order derivatives—known as the Hessian matrix—is obtained. The various combinations of its three eigenvalues, λ_1, λ_2, and λ_3, reflect the local structural features within the image, facilitating the identification of ball-like, line-like, or plate-like structures. The Frangi filter can detect the tubular characteristics of vasculature and is employed to enhance vascular structures, as shown in Equation (1), (2), (3).

$$R_b = \frac{|\lambda_1|}{\sqrt{|\lambda_2\lambda_3|}} \tag{1}$$

$$R_A = \frac{|\lambda_2|}{|\lambda_3|} \tag{2}$$

$$f(\sigma) = \begin{cases} 0, & if\,\lambda_2>0 or \lambda_3>0 \\ \left(1 - e^{-\frac{R_A^2}{0.5}}\right) e^{-\frac{R_B^2}{0.5}} \left(1 - e^{-\frac{S^2}{2c^2}}\right), & otherwise \end{cases} \tag{3}$$

Specifically, R_b quantifies the sphericity of the structure, while R_A is employed to distinguish between plate-like and line-like structures. The function f(σ) represents the vesselness scalar at each spatial point; the stronger the vesselness, the larger its value. After applying the Frangi filter to each spatial point, the vascular structures are enhanced, as illustrated in Figure 1c and d.

To further detect connected regions within the images, this study employed the bwconncomp function in MATLAB.[29] This function systematically identified connected regions of foreground pixels and classified them according to specified adjacency rules. Ultimately, regions connected to the primary mammary ductal structures were selected for three-dimensional reconstruction, generating model files in STL format using Geomagic software, as illustrated in Figure 1e and f. These model files were subsequently used for CFD analysis to investigate fluid dynamic and pharmacokinetic properties.

Pharmacokinetic Simulation Based on CFD

In this study, CFD was utilized to simulate the diffusion process of contrast agents within the body. The flow of bodily fluids is described by the incompressible Navier–Stokes equations, as shown in Equation (4), where is the velocity of the fluid, ρ is the density, and f represents the body force applied—in this case, gravity.

$$\rho(\partial u \partial t + u \cdot \nabla u) = -\nabla p + \mu \nabla^2 u + f \tag{4}$$

$$\nabla \cdot u = 0 \tag{5}$$

Considering the interactions between the two distinct fluid components—the contrast agent and the body fluids—this study adopted a convective diffusion model to describe the pharmacokinetics of the contrast agent. This model accounts for the two primary transport mechanisms of the contrast agent, as shown in Equation (6), where C denotes the concentration of the contrast agent.

$$\frac{\partial C}{\partial t} + = -\nabla \cdot (uC) + \nabla \cdot (D\nabla C) \tag{6}$$

In the equation (6), the left-hand side represents the rate of mass change per unit time at each point in the Eulerian coordinate system. The right-hand side comprises two terms: the convective term, which describes the transport of the contrast agent due to the bulk flow of bodily fluids (proportional to the product of fluid velocity and agent concentration), and the diffusion term, characterizing the agent's spontaneous molecular diffusion within the medium.

The three-dimensional computational model (STL format) was imported into ANSYS ICEM for mesh generation to facilitate numerical simulations. Subsequently, the governing equations were solved using ANSYS Fluent software.

To simulate the actual injection process of the contrast agent, a velocity inlet boundary condition was employed. It was assumed that the agent was uniformly injected over 10 seconds, with the inlet volume fraction set to 1 and the initial domain volume fraction set to 0. A pressure outlet boundary condition with a reference pressure of zero was specified. The simulation spanned 1,800 seconds with a time step of 0.1 seconds.

Results

The Safety of Animal Experiments

General View of Breast After Intraductal Perfusion

The gross changes of the breast in pigs and beagle dogs treated with intraductal chemotherapy were recorded. During perfusion, slight and transient swelling of the nipple treated with pegylated liposomal doxorubicin (PLD) occurred.

In the intraductal administration experiment of pigs, we found that there was only one mammary pore in the nipple of pigs, as shown in Figure 2A. Paclitaxel (albumin-bound) was perfused into the mammary ducts of pigs in the experimental group, and obvious swelling of the nipple of the experimental group could be observed immediately

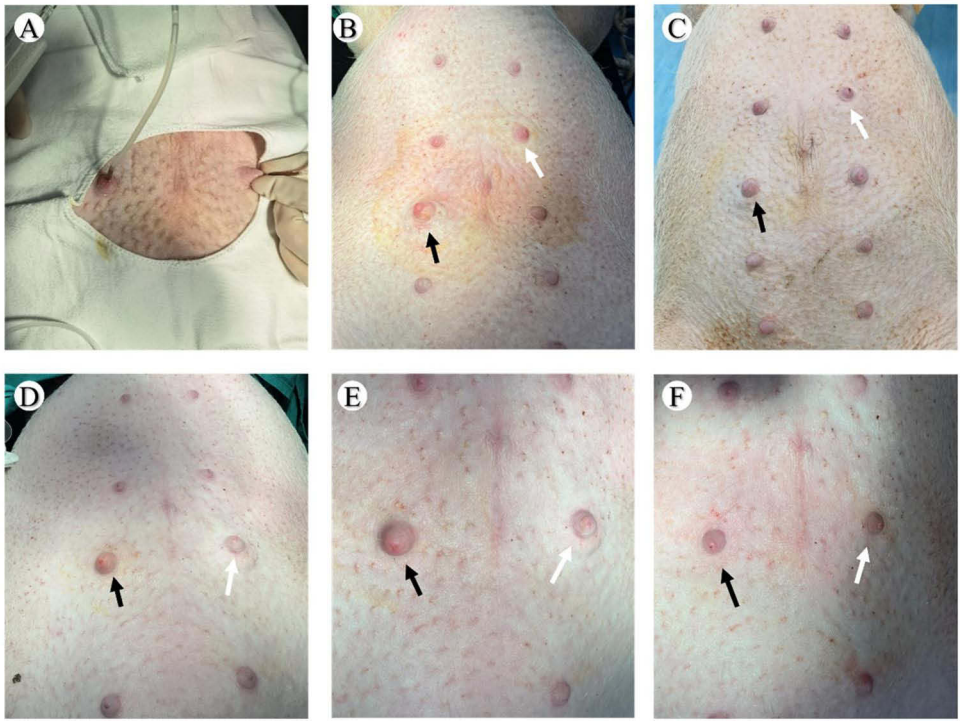

Figure 2 The changes of nipple and skin of pigs before and after infusion of PLD and paclitaxel (albumin-bound type). (**A**) Only one nipple hole could be reached in the nipple of pigs. (**B** and **C**) Paclitaxel (albumin-bound) group: (**B**) Immediately after the end of perfusion, the nipples in the experimental group were significantly swollen; (**C**) After 1 week of perfusion, the nipples of the experimental group and the control group returned to normal. (D~F) PLD group: (**D**) After 2 hours of perfusion, the nipples of both the experimental group and the control group were swollen, and the nipple swelling in the experimental group was more obvious. (**E**) After 1 week of perfusion, the nipple swelling in the experimental group was significantly relieved, and the subcutaneous area of the nipple in the control group was still swollen. (**F**) After 2 weeks of perfusion, the nipples of both the experimental group and the control group returned to normal. Black arrows refer to: nipples of the experimental group; The white arrow points to: the nipple of the control group.

https://doi.org/10.2147/BCTT.S547684

after the end of perfusion. After 1 week of perfusion, the nipple of the experimental group recovered to normal, and there was no significant difference between the experimental group and the control group, as shown in Figures 2B and C. 2h after PLD-perfusion in milk ducts of pigs in experimental group, swelling could be seen immediately in both experimental group and control group, and swelling was more obvious in experimental group. One week after perfusion, swelling in experimental group was obviously relieved, while subcutaneous area of control group was still swollen. Two weeks after perfusion, swelling in experimental group and control group returned to normal, as shown in Figures 2D–F.

The experimental group was perfused with PLD into the mammary ducts of dogs. The nipple of the experimental group was obviously inflamed during perfusion. After perfusion, the skin of the experimental group and surrounding breasts appeared slight erythema and swelling, as shown in Figures 3A and B. After perfusion for 1 week, the inflamed and swollen of the experimental group was relieved; after perfusion for 2 weeks, the nipples of the experimental group and the control group returned to normal, as shown in Figures 3C and D. In paclitaxel (albumin-bound) group, reddish swelling was observed immediately after perfusion in nipple of experimental group, similar to that in control group; after perfusion for 1 week, nipple of experimental group and control group returned to normal, as shown in Figures 3E and F.

Biodistribution of Doxorubicin

The biodistribution of doxorubicin on pig mammary gland.

Doxorubicin was detectable in the nipple and lactiferous duct, mammary tissue around the nipple and skin outside of the nipple as shown in Figure 4A–D, (H–J), but was not found in the remaining skin tissue, as shown in Figures 4E–G.

The biodistribution of doxorubicin on dog mammary gland.

Doxorubicin was not detectable in all biopsy samples.

Plasma Concentration of Doxorubicin

The plasma concentrations of doxorubicin were 4.46 μg/mL after the first perfusion and 8.02 μg/mL after the second perfusion in pig. The plasma concentrations of doxorubicin in beagle dog were 6.85 μg/mL and 1.60 μg/mL, respectively.

Outcome of the Patient's Treatment

A total of 2 subjects who were not suitable for systemic medication participated in the study between August 2021 and January 2022.

The Primary Lesion Was Significantly Reduced After Intraductal Perfusion

In case 1, the drug was administered into 4 ducts by intraductal perfusion apparatus, as shown in Figures 5A and B. Trastuzumab (150 mg) was then infused twice at 10 and 15 days before surgery, respectively, as shown in Table 1. The size of right breast mass significantly decreased 2 weeks after treatment, and the edema of the skin of the right breast subsided compared to before, as shown in Figures 6A and B. Breast singlephoton emission computed tomography imaging (SPECT) showed the irregular mass behind the right areola was significantly smaller than that before treatment. Imaging agent uptake was considerably reduced in multiple enlarged lymph nodes in the right axillary and pectoral muscle groups, as shown in Figures 7A–D. The plasma concentration of doxorubicin was about 800 times lower than that of normal intravenous administration, as shown in Figure 8. Doxorubicin was not detectable in the breast skin, submammary tissue, and tumor cells, but was clearly found in the nipple, large duct, supermammary tissue, and lymph nodes in the axilla, as shown in Figures 9A–H.

In case 2, the patient received a single intraductal infusion of doxorubicin, then treatment was abandoned for the patient's own reasons, as shown in Table 1. Although treatment was not completed, the CT scan taken in the patient's outpatient indicated that the lesion was smaller than before, and the patient reported pain relief.

Surgery After Local Treatment

A modified radical mastectomy was performed on the patient 1 after eight intraductal perfusions. The patient recovered well after surgery. The other patient discontinued the treatment and did not undergo surgery because of personal desire.

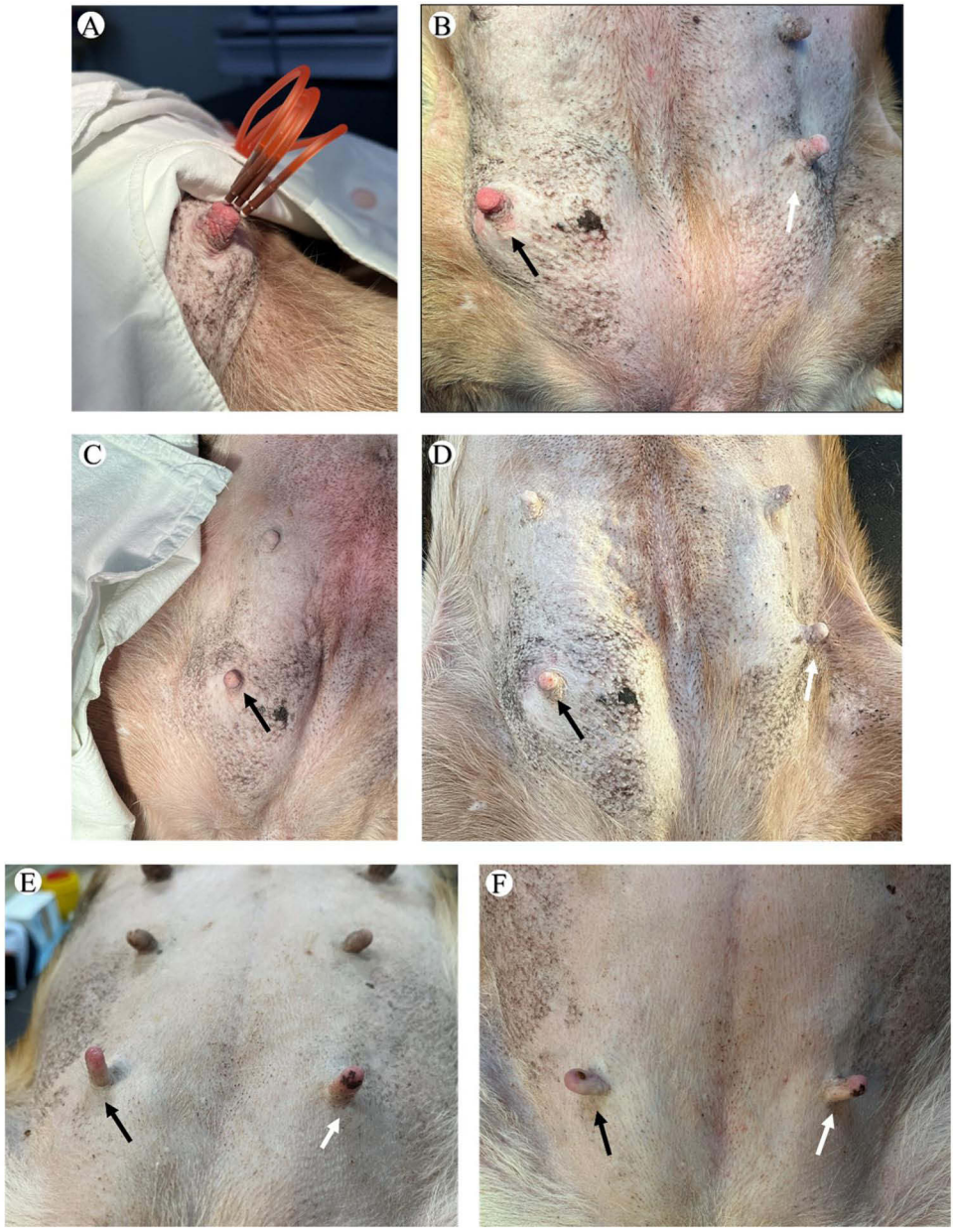

Figure 3 Nipple and skin changes before and after infusion of PLD and paclitaxel (albumin-bound type) in beagle dogs. (**A~D**) PLD group: (**A**) Nipple redness and swelling were obvious during intraductal perfusion; (**B**) Immediately after the end of perfusion, the nipples and surrounding breast skin were slightly erythema and swelling in the experimental group, and the nipples in the control group were slightly swollen. (**C**) After 1 week of perfusion, nipple redness and swelling in the experimental group were relieved; (**D**) After 2 weeks of perfusion, the nipples of both the experimental group and the control group returned to normal. (**E** and **F**) paclitaxel (albumin-bound) group: (**E**) Immediately after the end of perfusion, the nipples in the experimental group were slightly red and swollen, which was similar to that in the control group; (**F**) After 1 week of perfusion, the nipples of the experimental group and the control group returned to normal. Black arrows refer to: nipples of the experimental group; The white arrow points to: the nipple of the control group.

Pathological Evaluation

Preoperative multi-point hollow needle biopsy of case 1 showed grade 3 invasive ductal carcinoma with axillary lymph node metastasis, which was estrogen receptor (ER) negative, progesterone receptor (PR) negative and human epidermal factor receptor 2 (HER2) positive. Routine pathology after modified radical mastectomy showed breast invasive carcinoma, WHO III, Miller-Payne System Ib, axillary lymph node metastasis (13/18), right pectoral intermuscular lymph node metastasis (1/1).

https://doi.org/10.2147/BCTT.S547684

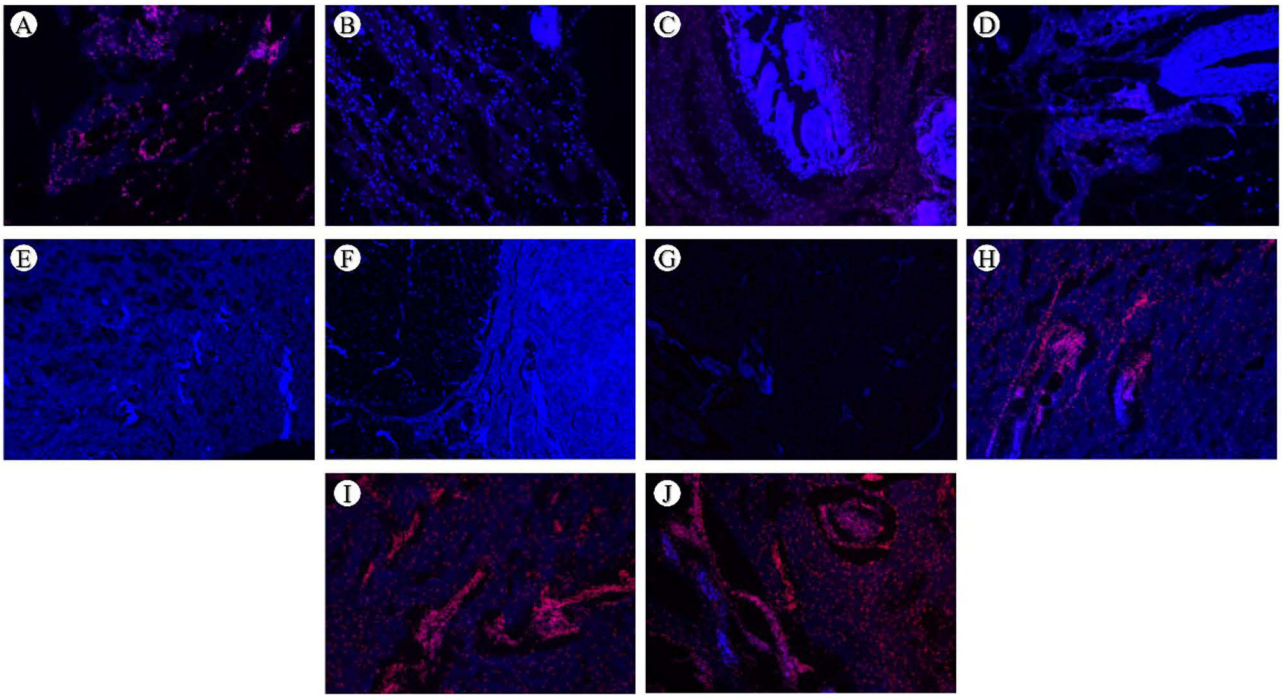

Figure 4 The tissues were stained with DAPI and the tissue distribution of doxorubicin was observed by confocal laser scanning microscopy. (**A**) Upper nipple glandular tissue, more doxorubicin distribution; (**B**) glandular tissue under the nipple, with a small amount of doxorubicin distributed; (**C**) Medial nipple glandular tissue, with a small amount of doxorubicin distributed; (**D**) lateral nipple gland tissue, with a small amount of doxorubicin distributed; (**E**) skin above the nipple, no doxorubicin distribution; (**F**) The skin below the nipple, no doxorubicin distribution was seen; (**G**) Medial nipple skin, no doxorubicin distribution; (**H**) Lateral papillae skin, with a small amount of doxorubicin distributed; (**I**) papillae, with a large distribution of doxorubicin; (**J**) Large milk duct behind the nipple, with a large amount of doxorubicin distributed. The magnification of A~D and H~J is 10×, and the magnification of E~G is 4×. The blue color is DAPI fluorescence and the red color is doxorubicin fluorescence.

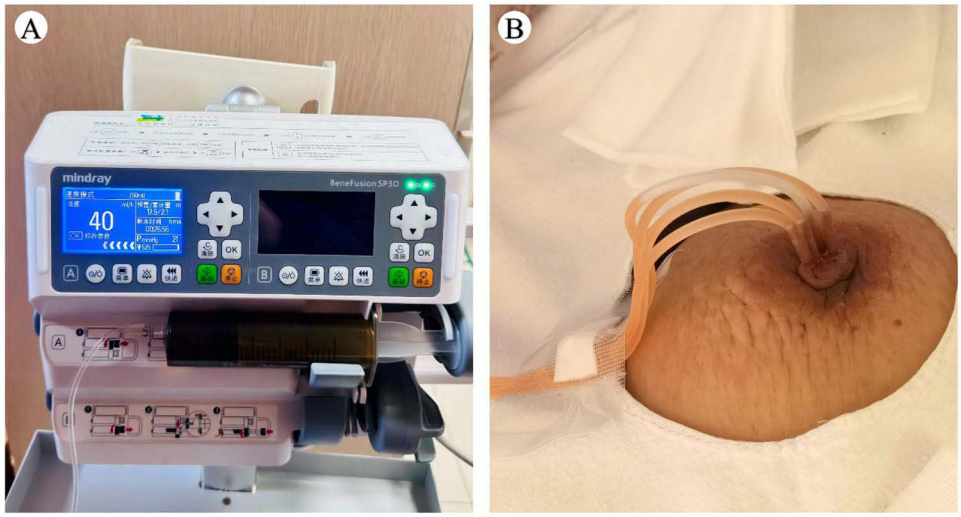

Figure 5 The process of injecting PLD through the breast tube using a syringe pump. (**A**) Fixed speed infusion pump device, and control the flow rate at 40mL/h. (**B**) Four mammary holes were selected near the cancer, and a catheter was inserted for intra-catheter infusion of drug treatment.

Results of Security Research

During treatment, the patient did not experience any digestive-related adverse events, and the problems associated with the cannulation of ducts and drug infusion were mild discomfort and transient swelling. No significant chemotherapy-related skin necrosis was observed in either patient. There were no abnormal changes of cardiac function in

Table 1 Treatment Options for 2 Patients with Locally Advanced Breast Cancer and Advanced Breast Cancer

Case	Date	PLD	Trastuzumab
Case 1	2021-08-26	2mg/20mL 5% Glucose solution	/
	2021-08-30	4mg/20mL 5% Glucose solution	/
	2021-09-01	8mg/20mL 5% Glucose solution	/
	2021-09-03	8mg/20mL 5% Glucose solution	/
	2021-09-10	/	150mg/10mL 0.9% Sodium chloride solution
	2021-09-13	10mg/15mL 5% Glucose solution	/
	2021-09-15	/	150mg/10mL 0.9% Sodium chloride solution
	2021-09-17	10mg/15mL 5% Glucose solution	/
Case 2	2022-01-06	2mg/20mL 5% Glucose solution	/

Electrocardiogram (ECG) and ultrasonic cardiogram (UCG). The results of blood routine and liver and kidney function test showed no side effects such as myelosuppression and liver function damage.

Result of Galactography and Pharmacokinetic Simulation in the Beagle Dog

In this study, numerical simulations were conducted to investigate the transport mechanisms of contrast agents within mammary ducts. The findings reveal that the propagation of the contrast agent primarily depends on two mechanisms: convective transport and molecular diffusion. Simulation results indicate that, in the initial phase post-injection, the transport of the contrast agent is predominantly governed by the pressure gradient of bodily fluids, resulting in directional flow. During this stage, convection serves as the principal transport mechanism, enabling the contrast agent to rapidly fill and reach the main ducts within 5 minutes, as shown in Figure 10. As the contrast agent reaches regions closest to the outlet, it begins to exit through the outlet, as illustrated by the streamline distribution in Figure 10.

In the subsequent stages following injection, the transport of the contrast agent in regions of the computational domain not directly reached by convection primarily relied on molecular diffusion mechanisms. Driven by the concentration gradient of the contrast agent, this mechanism facilitates spontaneous dispersion into the remaining parts of the computational domain, ultimately achieving complete filling of the entire structure within 25 minutes. Simulation results of this process also display the streamline distribution of the contrast agent within the computational domain, demonstrating that, aside from short-range convective transport, long-distance distribution is mainly accomplished through molecular diffusion.

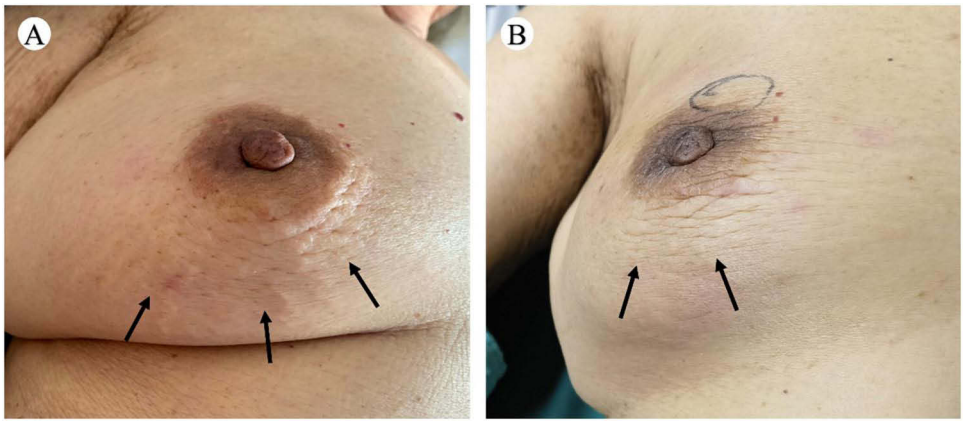

Figure 6 Periareolar skin changes before and after perfusion of case 1. (**A**) Before intraductal perfusion therapy, Orange peel changes of the breast skin and edema and thickening of the areola skin were seen at the arrows; (**B**) After perfusion therapy, the preoperative marking, the edema of the breast skin and the decrease of cellulite were seen at the arrows.

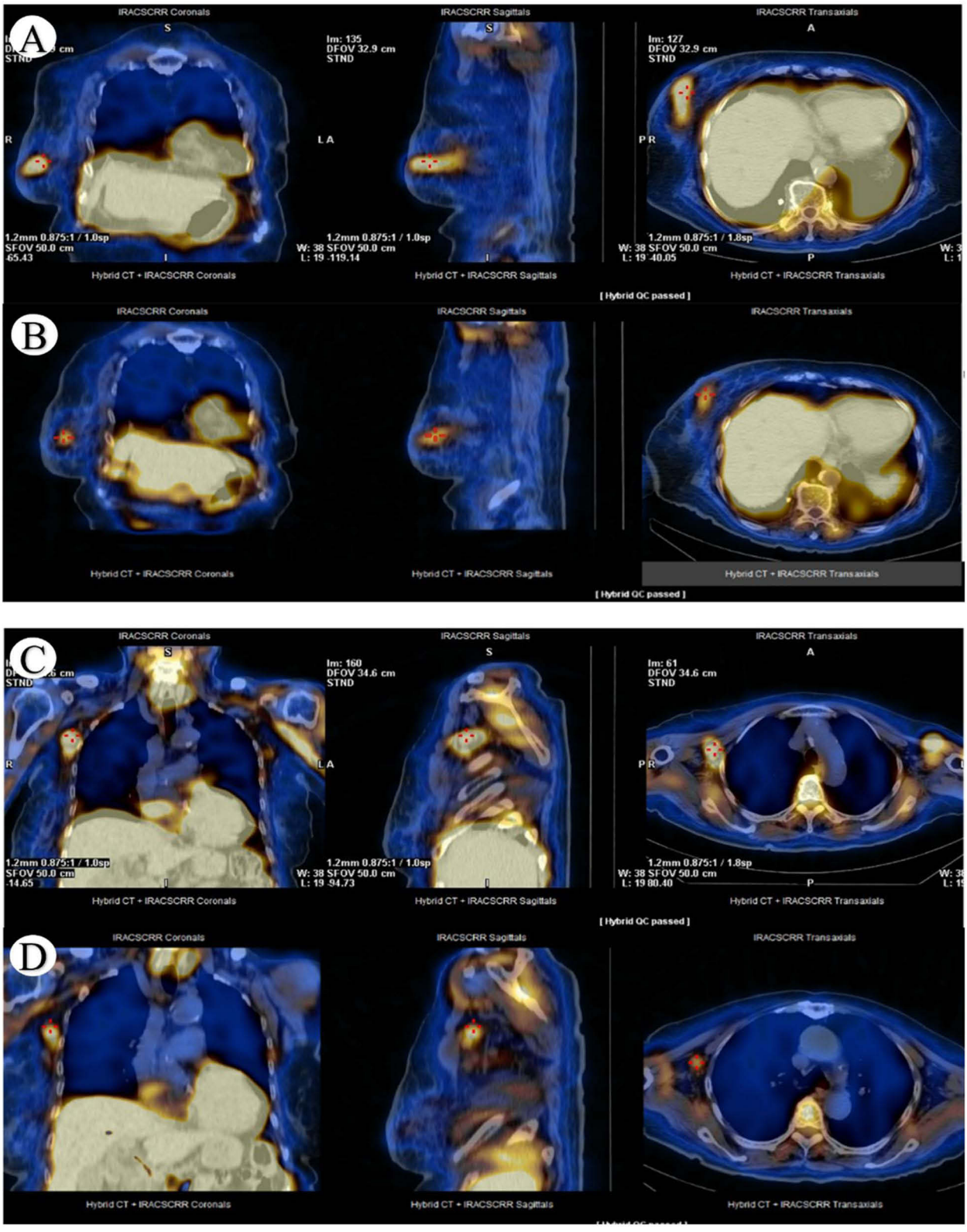

Figure 7 Comparison of SPECT images of the right post-areolar mass and multiple axillary and pectoral muscle nodes in different profiles of case 1 before and after intraductal perfusion therapy. (**A**) Coronal, sagittal and horizontal images of the right postareolar irregular mass before treatment; (**B**) Coronal, sagittal and horizontal images of the treated right post-areolar irregular mass; (**C**) Coronal, sagittal and horizontal images of multiple swollen lymph nodes in the right axillary and pectoral muscles before treatment; (**D**) Coronal, sagittal and horizontal images of multiple swollen lymph nodes in the right axillary and pectoral muscles after treatment. After treatment, the right post-areolar mass and multiple enlarged lymph nodes in the axilla and pectoral muscles were smaller than those before treatment.

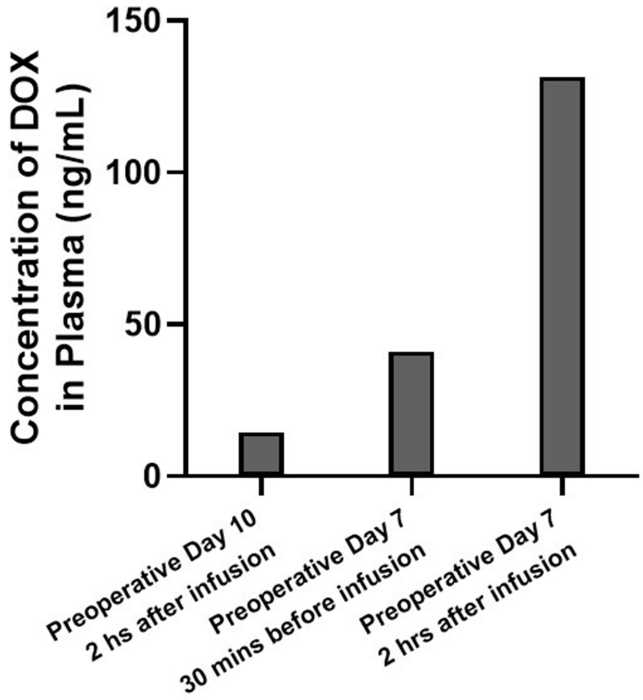

Figure 8 DOX plasma drug concentrations were determined by LC-MS/MS method.

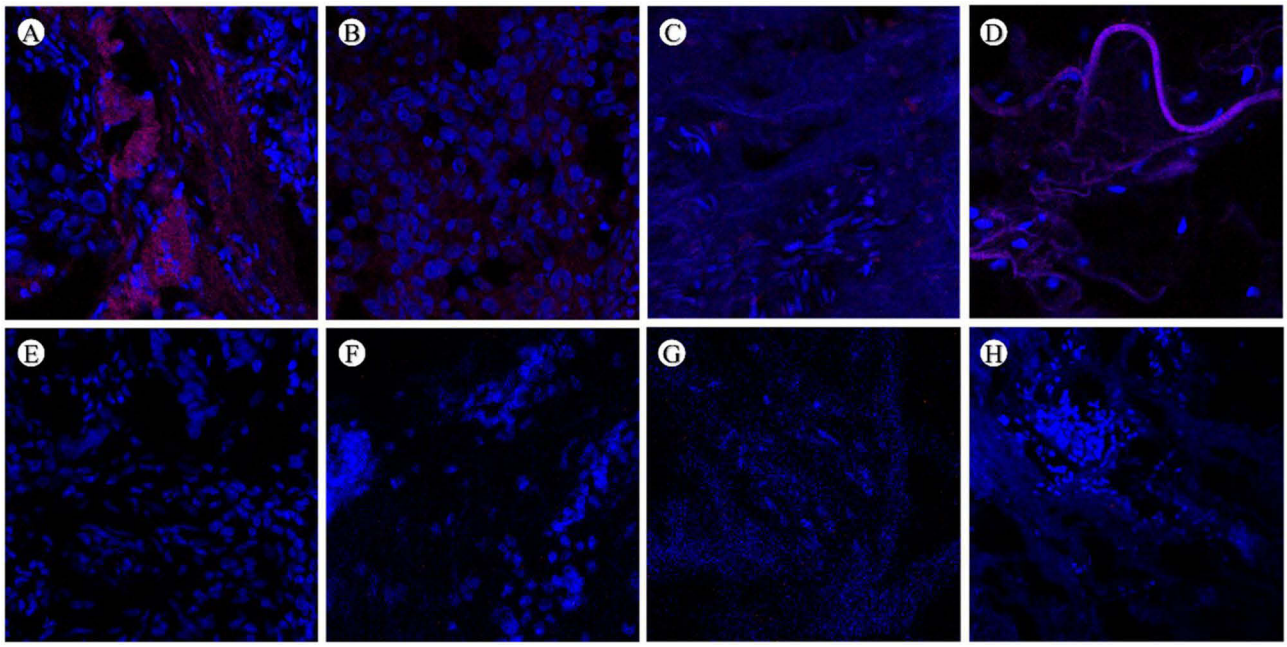

Figure 9 The tissues were stained with DAPI and the biodistribution of doxorubicin was observed by confocal laser scanning microscopy. (**A**) Large milk duct on the right side, with more doxorubicin distribution; (**B**) Group III lymph nodes in the right axilla, with a small amount of doxorubicin distributed; (**C**) Right nipple with a small amount of doxorubicin distributed; (**D**) Upper quadrant mammary gland tissue of the right breast, with more doxorubicin distribution; (**E**) Group I lymph nodes in the right axilla, with a small amount of doxorubicin distributed; (**F**) The skin of the right breast, the distribution of doxorubicin is not observed; (**G**) tumor tissue, no doxorubicin distribution observed; (**H**) Breast tissue in the right submammary quadrant, no doxorubicin distribution was observed. The A~G magnification is 40×, and the H magnification is 20×. The blue color is DAPI fluorescence and the red color is doxorubicin fluorescence.

https://doi.org/10.2147/BCTT.S547684

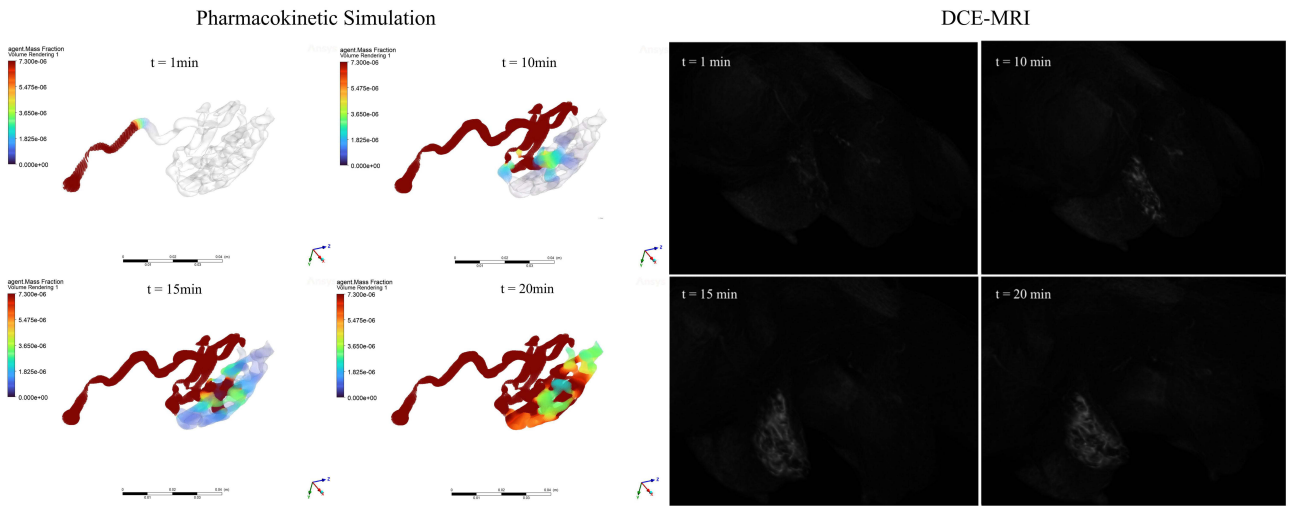

Figure 10 Comparison of the simulated transport processes of the contrast agent at different time points with DCE-MRI images.

Therefore, the transport of the contrast agent within mammary ducts could be summarized into two main stages: initially, rapid filling of nearby main ducts and adjacent regions predominantly through convection; subsequently, filling of the entire structure via molecular diffusion mechanisms. While convective transport was highly efficient, its effective range was limited to areas proximal to the main ducts. In contrast, molecular diffusion, although slower, ensured uniform distribution of the contrast agent throughout the entire mammary duct system.

Pressure analysis concurrently validated this conclusion. In the main and branch duct regions traversed by streamlines, wall and volume renderings exhibited negative pressure zones, as shown in Figure 11. It is noteworthy that, since the reference pressure at the outlet is set to zero, the negative pressure here indicates that the pressure is lower than at the

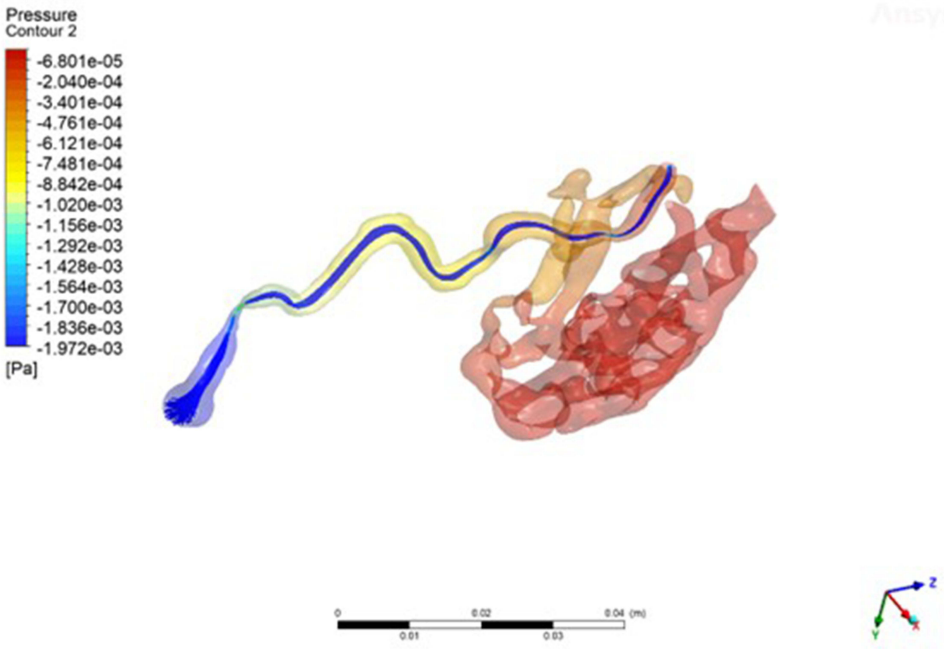

Figure 11 Pressure contour plots of the wall surface and the streamlines are presented. The regions through which the streamlines pass correspond to areas of negative pressure. At this point, the transport direction is opposite to the direction of the pressure gradient, indicating that the drug is being transported by diffusion under the influence of the concentration gradient.

outlet and other regions. Combined with Bernoulli's principle, this suggests the presence of directional flow in the low-pressure regions. The coincidence of low-pressure zones with areas crossed by streamlines further verifies that convective transport of the contrast agent occurs in these regions.

Discussion

LABC is usually defined as clinical stage III disease, such as primary tumor ≥5cm or T0–T3 primary tumors with regional lymph node metastasis. Skin invasion is also included. Both large operable and locally advanced inoperable tumors are preferred for systemic treatment.[6] The standard treatment for LABC is to first shrink or degrade the tumor with neoadjuvant treatment, mainly chemotherapy, and then reevaluate the surgery. But for older women, preoperative chemotherapy can be a challenge.[30–32] At present, chemotherapy for cancer is mainly administered by oral or intravenous administration. Besides treating cancer, systemic administration can also damage other normal tissues, leading to some harmful side effects. The NCCN guidelines for Older Adult Oncology provides specific practical framework for the use of comprehensive geriatric assessment when evaluating older adults with cancer.[33] Scientists from a multi-disciplinary field are working together to promote in situ drug delivery techniques such as the fusion of biomaterials and the construction of suitable nanohydrogel composite systems that may be used to treat LABC.[15] The FeDeriCa study suggested that the combination of subcutaneous pertuzumab and trastuzumab had the same pathologic complete response rate as intravenous administration in neoadjuvant therapy.[16] Liposomal doxorubicin was subcutaneously injected into the 4T1 xenograft model and was released at the tumor site, thereby enhancing antitumor effects and reducing off-target effects.[34] Ductal lavage, that is, intubation at the nipple catheter opening, saline lavage allows for fluid examination. Direct delivery of therapeutic drugs through catheters is possible.[18] We treated non-lactation mastitis well with the infusion of antibiotics and dexamethasone using milk duct technique. Therefore, it was inspired that breast cancer may be treated with liposomal doxorubicin and trastuzumab injected through the large ducts of the nipple.

The feasibility of intraductal administration has been demonstrated in a number of preclinical studies.[17,35–38] In the study of Stearns et al,[17] the efficacy of intraductal administration with five chemotherapy drugs in the MNU-induced rat model was evaluated, which confirmed all five drugs significantly inhibited breast cancer compared with intravenous administration without significant toxic effects. Based on the preclinical study, there was a reason to believe that intraductal chemotherapy is a feasible treatment for breast cancer. To verify the safety of intraductal perfusion, we selected large mammal breast models (pigs and dogs) for the experiment. In the pig mammary gland, the drug can be distributed to the glandular tissue of the breast by intraductal perfusion and can be detected. The distribution of doxorubicin detected in the skin in the lateral quadrant of the nipple may be due to drug overflow during perfusion or to local catheter penetration during intubation leading to drug delivery to the skin. However, no significant skin necrosis was observed after perfusion, which may be related to local drug concentrations or animal skin characteristics. In the pigs' experiment process, we found that the skin of pigs was rough, the breast was small and there was only a nipple hole in each nipple of breast. In order to better simulate the perfusion in the human breast, Beagles with more ductal openings were selected for the second animal experiment. The Beagle's nipple has multiple orifices, and the mammary gland consists of alveoli and ducts, which are more closely related to the structure of human breast. In the beagle dog experiment, the distribution of doxorubicin was not detected in breast tissue, probably because the biopsy tissue was not taken correctly, which needed further improvement. At the same time, the drug distribution in the skin was undetectable, suggesting that catheter perfusion was relatively safe. Overall, no necrosis was observed in two animal experiments.

Stearns et al[17] also conducted a clinical trial with 15 invasive breast carcinoma awaiting mastectomy, which successfully administered intraductal chemotherapy with no serious adverse events. Doxorubicin was not detected in the plasma of patients who received intraductal perfusion, whereas low concentrations of doxorubicin were detected in breast tissue in only one of the three patients who received intravenous PLD. These results were consistent with our clinical case exploratory study. However, the study of Stearns et al still had certain limitations. As a neoadjuvant chemotherapy for breast cancer, PLD usually requires multiple cycles of treatment, and the adverse reactions associated with it are usually dose-dependent. This trial injected PLD into the breast catheter system once and lacked observation of adverse reactions caused by cumulative drug doses. Moreover, this trial performed mastectomy 1 week after administration, did not dynamically monitor PLD-related skin damage, and lacked an assessment of the medium and long-term

safety of intraductal administration. In our clinical case exploratory study, Case 1 was treated with a total of 8 intramammary intraductal infusion treatments (6 PLD infusions and 2 trastuzumab infusions). During this period, changes in the nipple and breast skin were closely monitored. During follow-up to 2 months after surgery, no significant skin toxicity was observed. Case 1 was a patient with locally advanced breast cancer who could not tolerate systemic chemotherapy and was inoperable. After re-examination of breast SPECT after intraductal infusion treatment, it was found that the primary tumor focuses and axillary lymph nodes had significantly shrunk, and the complaint of local pain was significantly relieved. In addition, the patient successfully underwent modified radical mastectomy for breast cancer after perfusion therapy and recovered well postoperatively. Some tissues of breast specimens were taken after the operation to determine the drug distribution. We did not observe the distribution of doxorubicin in the skin, tumor tissue, or breast tissue under the nipple. Since the sampling of tumor tissue mainly relies on the experience of the surgeon for naked judgment, sampling errors may occur, and the distribution of doxorubicin is not detected. To our surprise, the patient's enlarged axillary lymph nodes shrank after perfusion, and doxorubicin could also be seen in the axillary lymph node tissue. We believe this is because the drug enters the mammary duct and spreads to the lymphatic system with tumor cells to reach the axillary lymph nodes to play an anti-tumor effect. From this, we suspect that intramammary infusion of chemotherapeutic drugs is not limited to the treatment of ductal carcinoma in situ (DCIS) or invasive ductal carcinoma. We need more research to prove this conjecture. In Case 1, the plasma drug concentration measured after intramammary duct infusion was much lower than that during intravenous injection, which means that the systemic exposure of the chemotherapeutic drugs is less, resulting in lower systemic toxicity, and is less likely to cause systemic adverse reactions. As we expected, this elderly patient did not experience hematological toxicities such as granulocytopenia, decreased platelets and hemoglobin, nor liver and kidney toxicities such as abnormal liver and kidney function, nor gastrointestinal adverse reactions such as nausea and vomiting, and did not experience cardiac toxicity such as decreased cardiac ejection fraction or abnormal ECG changes during intraductal infusion of chemotherapy drugs. Therefore, we think that intraductal treatment of locally advanced breast cancer is relatively feasible and safe.

Currently, some clinical studies on intraductal infusion of chemotherapeutic drugs advocate that this local treatment strategy can be used as a "chemical mastectomy" to prevent or early treat breast cancer. However, Chun et al[39] found that long-term intraductal PLD infusion may increase the risk of malignant tumors, a finding that almost ruled out the possibility of intraductal PLD infusion being clinically used to treat or prevent early breast cancer. Our study mainly considered the application of intramammary perfusion therapy to locally advanced or advanced breast cancer. By controlling the local breast lesions of breast cancer, the inoperable breast cancer can be reduced and reduced, and surgical resection can be performed after reaching operable standards. Improve the patient's quality of life and extend the patient's expected survival time.

In this study, gadolinium meglumine injection was used to enhance MRI in the mammary gland of contrast dogs, and the drug delivery pathway was revealed. Through the combination of threshold segmentation technology and Frangi filter, the features of breast duct were extracted successfully. Subsequently, the process of drug transport and metabolism was simulated by CFD technology, and compared with the actual MRI images to verify the accuracy of the simulation model. The results showed that the transport of contrast medium in mammary duct mainly depended on convection and diffusion, in which the transport efficiency of convection mechanism was significantly higher than that of diffusion mechanism. According to the transport mechanism of the contrast medium, the milk duct structure could be divided into two different regions: one area was transported rapidly through the convection mechanism, and the other part mainly depended on the diffusion mechanism, and the transport speed was relatively slow. This discovery provided an important basis for the design of an efficient anticancer drug delivery system, especially in the realization of targeted treatment and accurate medical care. Through identifying high-speed transport pathways, it was helpful to improve the efficiency and effectiveness of drug delivery. The computational model established in this study not only successfully revealed the transport mechanism of contrast media in complex structures but also provided a valuable theoretical and computational basis for the selection of anticancer drug delivery pathway and pharmacokinetic analysis. It provided a new perspective for the design of future drug delivery system and the optimization of cancer treatment strategy.

With these promising results, however, there are still many problems need to be solved in the clinical application of intraductal therapy. The anatomy of the breast is not well understood, and it is difficult to localize the orifice of the breast

duct where the tumor is located. There are approximately 5 to 27 separate ductal systems in each breast, each of which is intertwined.[40] The number of orifices may also affect the perfusion effect. The mammary duct orifice adjacent to the tumor may be selected for perfusion, but further studies are needed to elucidate the anatomy for more precise treatment. Because of the limited intraductal volume, it is difficult to determine the dose of drugs and set the perfusion pressure. We were concerned about whether tumor cells would spread through perfusion dynamics after perfusion. In the patient who completed surgery after perfusion, no tumor cells were found in normal tissues. In addition, doxorubicin was also detected in the axillary lymph nodes of the patient. At present, our conclusions about the efficacy of Adriamycin in local applications are hypothetical. This study focuses on the feasibility and safety of intramammary infusion chemotherapy in patients with LABC. For the route and mechanism of doxorubicin diffusion in mammary duct, we need to conduct more in-depth research to further clarify.

Although the computational model developed in this study showed some effectiveness in the preliminary application, there are some limitations that need to be further improved. First of all, there is a lack of accurate quantitative relationship between contrast medium concentration and MRI image gray value in the current model, which limits the ability of accurate quantitative verification and calibration based on image gray value. In addition, the sample size used in this study is small, and more samples should be included in the future study to improve the representativeness and accuracy of the study. Finally, when simulating the delivery of contrast media in breast ducts, it is assumed that the density and kinetic viscosity of body fluids are equal to those of plasma. However, in practice, the composition of body fluid in the breast duct is more complex, although its physical parameters are similar to those of plasma, but there are still differences. In the future, further experiments are needed to analyze the chemical composition and physical properties of the body fluid in the milk duct for calibration and undetermined model.

In conclusion, we tested the safety of intraductal chemotherapy. Moreover, the successful establishment of the calculation model revealed the delivery mechanism of contrast medium in the breast duct system, which provided a valuable theoretical and computational basis for the selection of anticancer drug delivery pathway and pharmacokinetic analysis. However, the formulation of specific programs needs to be further studied. Because the pathophysiological conditions of the healthy animal model used in this study are different from those of breast cancer patients, and the CFD model is different from the real tumor environment, the current conclusions are primarily applicable under ideal conditions with patent ducts and that effectiveness in advanced breast cancer patients requires further investigation. There are many challenges to the management of the therapy of LABC. In the later stage, it is still necessary to expand the sample size and strict trial design to further explore the effect and safety of intraductal infusion of chemotherapeutic drugs in the treatment of local breast lesions of breast cancer. In addition, advanced techniques such as mass spectrometry imaging will be used in future studies to quantitatively analyze drug distribution in tumor tissues.

Ethical Statement

The Shanghai Pudong Hospital Ethics Committee was approved this study (No. QWJWZY-01). The authors envisaged all standard protocols in accordance with the 1964 Declaration of Helsinki.

Acknowledgments

The study was supported by (1) Funded by Key Discipline Construction Project SHXHZDXK: 202313, China of Shanghai Xuhui Health System. Department: General surgery of Shanghai Eighth People's Hospital, Shanghai 200235, China. Dress: No. 8 Caobao Road, Xuhui District, Shanghai, China. (2) Funded by Research Grant for Health Science and Technology of Pudong Municipal Commission of Health committee of Shanghai (Grant No.PW2023A-62). (3) Funded by the Scientific Research Foundation provided by Pudong Hospital affiliated to Fudan University (Project no. YJDXB2023-06). (4) Funded by the Scientific Research Foundation provided by Pudong Hospital affiliated to Fudan University (Project no. YJ2023-03).

Disclosure

The authors report no conflicts of interest in this work.

References

1. Sung H, Ferlay J, Siegel RL, et al. Global cancer statistics 2020: GLOBOCAN estimates of incidence and mortality worldwide for 36 cancers in 185 countries. *CA Cancer J Clin*. 2021;71:209–249. doi:10.3322/caac.21660
2. Smith BD, Smith GL, Hurria A, Hortobagyi GN, Buchholz TA. Future of cancer incidence in the United States: burdens upon an aging, changing nation. *J Clin Oncol off J Am Soc Clin Oncol*. 2009;27:2758–2765. doi:10.1200/JCO.2008.20.8983
3. Harbeck N, Gnant M. Breast cancer. *Lancet Lond Engl*. 2017;389:1134–1150. doi:10.1016/S0140-6736(16)31891-8
4. Siegel RL, Miller KD, Wagle NS, Jemal A. Cancer statistics, 2023. *CA Cancer J Clin*. 2023;73:17–48. doi:10.3322/caac.21763
5. Allemani C, Sant M, Weir HK, et al. Breast cancer survival in the US and Europe: a concord high-resolution study. *Int J Cancer*. 2013;132:1170–1181. doi:10.1002/ijc.27725
6. Tryfonidis K, Senkus E, Cardoso MJ, Cardoso F. Management of locally advanced breast cancer-perspectives and future directions. *Nat Rev Clin Oncol*. 2015;12:147–162. doi:10.1038/nrclinonc.2015.13
7. Bear HD, Anderson S, Smith RE, et al. Sequential preoperative or postoperative docetaxel added to preoperative doxorubicin plus cyclophosphamide for operable breast cancer: national surgical adjuvant breast and bowel project protocol B-27. *J Clin Oncol off J Am Soc Clin Oncol*. 2006;24:2019–2027. doi:10.1200/JCO.2005.04.1665
8. Gianni L, Pienkowski T, Im Y-H, et al. Efficacy and safety of neoadjuvant pertuzumab and trastuzumab in women with locally advanced, inflammatory, or early HER2-positive breast cancer (NeoSphere): a randomised multicentre, open-label, Phase 2 trial. *Lancet Oncol*. 2012;13:25–32. doi:10.1016/S1470-2045(11)70336-9
9. Loibl S, O'Shaughnessy J, Untch M, et al. Addition of the PARP inhibitor veliparib plus carboplatin or carboplatin alone to standard neoadjuvant chemotherapy in triple-negative breast cancer (BrighTNess): a randomised, Phase 3 trial. *Lancet Oncol*. 2018;19:497–509. doi:10.1016/S1470-2045(18)30111-6
10. Johnston SRD, Harbeck N, Hegg R, et al. Abemaciclib combined with endocrine therapy for the adjuvant treatment of HR+, HER2-, node-positive, high-risk, early breast cancer (monarchE). *J Clin Oncol off J Am Soc Clin Oncol*. 2020;38:3987–3998. doi:10.1200/JCO.20.02514
11. Schmid P, Cortes J, Pusztai L, et al. Pembrolizumab for early triple-negative breast cancer. *N Engl J Med*. 2020;382:810–821. doi:10.1056/NEJMoa1910549
12. Clarke M, et al. Effects of radiotherapy and of differences in the extent of surgery for early breast cancer on local recurrence and 15-year survival: an overview of the randomised trials. *Lancet Lond Engl*. 2005;366:2087–2106.
13. Mladěnka P, Applová L, Patočka J, et al. Comprehensive review of cardiovascular toxicity of drugs and related agents. *Med Res Rev*. 2018;38:1332–1403. doi:10.1002/med.21476
14. Zamorano JL, Lancellotti P, Rodriguez Muñoz D, et al. ESC position paper on cancer treatments and cardiovascular toxicity developed under the auspices of the ESC committee for practice guidelines: the task force for cancer treatments and cardiovascular toxicity of the European society of cardiology (ESC). *Eur Heart J*. 2016;37:2768–2801. doi:10.1093/eurheartj/ehw211
15. Tang R-Z, Liu -Z-Z, Gu -S-S, Liu X-Q. Multiple local therapeutics based on nano-hydrogel composites in breast cancer treatment. *J Mater Chem B*. 2021;9:1521–1535. doi:10.1039/D0TB02737E
16. Tan AR, Im S-A, Mattar A, et al. Fixed-dose combination of pertuzumab and trastuzumab for subcutaneous injection plus chemotherapy in HER2-positive early breast cancer (FeDeriCa): a randomised, open-label, multicentre, non-inferiority, phase 3 study. *Lancet Oncol*. 2021;22:85–97. doi:10.1016/S1470-2045(20)30536-2
17. Stearns V, Mori T, Jacobs LK, et al. Preclinical and clinical evaluation of intraductally administered agents in early breast cancer. *Sci Transl Med*. 2011;3:106ra108. doi:10.1126/scitranslmed.3002368
18. Khan SA, Baird C, Staradub VL, Morrow M. Ductal lavage and ductoscopy: the opportunities and the limitations. *Clin Breast Cancer*. 2002;3:185–191. doi:10.3816/CBC.2002.n.022
19. King BL, Love SM. The intraductal approach to the breast: raison d'être. *Breast Cancer Res BCR*. 2006;8:206. doi:10.1186/bcr1410
20. Chen K, Zhu L, Hu T, et al. Ductal lavage for patients with nonlactational mastitis: a single-arm, proof-of-concept trial. *J Surg Res*. 2019;235:440–446. doi:10.1016/j.jss.2018.10.023
21. Twelves D, Nerurkar A, Osin P, et al. The anatomy of fluid-yielding ducts in breast cancer. *Breast Cancer Res Treat*. 2012;132:555–564. doi:10.1007/s10549-011-1623-y
22. Love SM, Zhang W, Gordon EJ, et al. A feasibility study of the intraductal administration of chemotherapy. *Cancer Prev Res Phila Pa*. 2013;6:51–58. doi:10.1158/1940-6207.CAPR-12-0228
23. Negin Mortazavi S, Geddes D, Hassanipour F. Lactation in the human breast from a fluid dynamics point of view. *J Biomech Eng*. 2017;139. doi:10.1115/1.4034995
24. Shipley RJ, Sweeney PW, Chapman SJ, Roose T. A four-compartment multiscale model of fluid and drug distribution in vascular tumours. *Int J Numer Methods Biomed Eng*. 2020;36:e3315. doi:10.1002/cnm.3315
25. Wu C, Pineda F, Hormuth DA, Karczmar GS, Yankeelov TE. Quantitative analysis of vascular properties derived from ultrafast DCE-MRI to discriminate malignant and benign breast tumors. *Magn Reson Med*. 2019;81:2147–2160. doi:10.1002/mrm.27529
26. Wu C, Hormuth DA, Oliver TA, et al. Patient-specific characterization of breast cancer hemodynamics using image-guided computational fluid dynamics. *IEEE Trans Med Imaging*. 2020;39:2760–2771. doi:10.1109/TMI.2020.2975375
27. Wu C, Hormuth DA, Lorenzo G, et al. Towards patient-specific optimization of neoadjuvant treatment protocols for breast cancer based on image-guided fluid dynamics. *IEEE Trans Biomed Eng*. 2022;69:3334–3344. doi:10.1109/TBME.2022.3168402
28. Korde LA, Somerfield MR, Carey LA, et al. Neoadjuvant chemotherapy, endocrine therapy, and targeted therapy for breast cancer: ASCO guideline. *J Clin Oncol off J Am Soc Clin Oncol*. 2021;39:1485–1505. doi:10.1200/JCO.20.03399
29. Li W, Liu J, Xiao C, et al. A fast forward 3D connection algorithm for mitochondria and synapse segmentations from serial EM images. *BioData Min*. 2018;11:24. doi:10.1186/s13040-018-0183-7
30. Dhanushkodi M, Sridevi V, Shanta V, et al. Locally advanced breast cancer (LABC): real-world outcome of patients from cancer institute, Chennai. *JCO Glob Oncol*. 2021;7:767–781. doi:10.1200/GO.21.00001
31. Gosain R, Pollock Y, Jain D. Age-related disparity: breast cancer in the elderly. *Curr Oncol Rep*. 2016;18:69. doi:10.1007/s11912-016-0551-8

32. Biganzoli L, Wildiers H, Oakman C, et al. Management of elderly patients with breast cancer: updated recommendations of the international society of geriatric oncology (SIOG) and European society of breast cancer specialists (EUSOMA). *Lancet Oncol*. 2012;13:e148–e160. doi:10.1016/S1470-2045(11)70383-7
33. Dotan E, Walter LC, Browner IS, et al. NCCN guidelines® insights: older adult oncology, version 1.2021. *J Natl Compr Cancer Netw JNCCN*. 2021;19:1006–1019. doi:10.6004/jnccn.2021.0043
34. An D, Yu X, Jiang L, et al. Reversal of Multidrug resistance by apolipoprotein a1-modified doxorubicin liposome for breast cancer treatment. *Mol*. 2021;26.
35. Okugawa H, Yamamoto D, Uemura Y, et al. Effect of perductal paclitaxel exposure on the development of MNU-induced mammary carcinoma in female S-D rats. *Breast Cancer Res Treat*. 2005;91:29–34. doi:10.1007/s10549-004-6455-6
36. Murata S, Kominsky SL, Vali M, et al. Ductal access for prevention and therapy of mammary tumors. *Cancer Res*. 2006;66:638–645. doi:10.1158/0008-5472.CAN-05-4329
37. Gao D, Liu J, Yuan J, et al. Intraductal administration of N-methyl-N-nitrosourea as a novel rodent mammary tumor model. *Ann Transl Med*. 2021;9:576. doi:10.21037/atm-21-1540
38. Wang G, Chen C, Pai P, et al. Intraductal fulvestrant for therapy of ERα-positive ductal carcinoma in situ of the breast: a preclinical study. *Carcinogenesis*. 2019;40:903–913. doi:10.1093/carcin/bgz084
39. Chun YS, Yoshida T, Mori T, et al. Intraductally administered pegylated liposomal doxorubicin reduces mammary stem cell function in the mammary gland but in the long term, induces malignant tumors. *Breast Cancer Res Treat*. 2012;135:201–208. doi:10.1007/s10549-012-2138-x
40. Wang G, Kumar A, Ding W, et al. Intraductal administration of transferrin receptor-targeted immunotoxin clears ductal carcinoma in situ in mouse models of breast cancer-a preclinical study. *Proc Natl Acad Sci USA*. 2022;119:e2200200119. doi:10.1073/pnas.2200200119